



Article scientifique

Article

2021

Published version

Open Access

This is the published version of the publication, made available in accordance with the publisher's policy.

---

## Disrupted resting-state EEG alpha-band interactions as a novel marker for the severity of visual field deficits after brain lesion

---

Allaman, Leslie; Mottaz, Anais; Guggisberg, Adrian

### How to cite

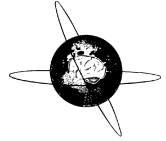
ALLAMAN, Leslie, MOTTAZ, Anais, GUGGISBERG, Adrian. Disrupted resting-state EEG alpha-band interactions as a novel marker for the severity of visual field deficits after brain lesion. In: Clinical neurophysiology, 2021, vol. 132, n° 9, p. 2101–2109. doi: 10.1016/j.clinph.2021.05.029

This publication URL: <https://archive-ouverte.unige.ch/unige:177864>

Publication DOI: [10.1016/j.clinph.2021.05.029](https://doi.org/10.1016/j.clinph.2021.05.029)

© The author(s). This work is licensed under a Creative Commons Attribution (CC BY 4.0)

<https://creativecommons.org/licenses/by/4.0>



# Disrupted resting-state EEG alpha-band interactions as a novel marker for the severity of visual field deficits after brain lesion



Leslie Allaman, Anaïs Mottaz, Adrian G. Guggisberg\*

Division of Neurorehabilitation, Department of Clinical Neurosciences, University Hospital of Geneva, Av. de Beau-Séjour 26, 1211 Genève 14, Switzerland

## ARTICLE INFO

### Article history:

Accepted 25 May 2021

Available online 28 June 2021

### Keywords:

Homonymous visual field deficit

Functional connectivity

Alpha-band

Task-induced activation

## HIGHLIGHTS

- Visual field deficits are related to reduced task-related activations and spontaneous coupling in the alpha-band.
- Spontaneous  $\alpha$ -band interactions are the best predictor of deficit among these two markers.
- Spontaneous  $\alpha$ -band coupling of ipsilesional visual areas could be a target for rehabilitation.

## ABSTRACT

**Objective:** Homonymous visual field deficits (HFVDs) are frequent following brain lesions. Current restoration treatments aim at activating areas of residual vision through numerous stimuli, but show limited effect. Recent findings suggest that spontaneous neural  $\alpha$ -band coupling is more efficient for enabling visual perception in healthy humans than task-induced activations. Here, we evaluated whether it is also associated with the severity of HFVD.

**Methods:** Ten patients with HFVDs after brain damage in the subacute to chronic stage and ten matched healthy controls underwent visual stimulation with alternating checkerboards and electroencephalography recordings of stimulation-induced power changes and of spontaneous neural interactions during rest.

**Results:** Visual areas of the affected hemisphere showed reduced event-related power decrease in  $\alpha$  and  $\beta$  frequency bands, but also reduced spontaneous  $\alpha$ -band interactions during rest, as compared to contralateral areas and healthy controls. A multivariate stepwise regression retained the degree of disruption of spontaneous interactions, but not the reduced task-induced power changes as predictor for the severity of the visual deficit.

**Conclusions:** Spontaneous  $\alpha$ -band interactions of visual areas appear as a better marker for the severity of HFVDs than task-induced activations.

**Significance:** Treatment attempts of HFVDs should try to enhance spontaneous  $\alpha$ -band coupling of structurally intact ipsilesional areas.

© 2021 International Federation of Clinical Neurophysiology. Published by Elsevier B.V. This is an open access article under the CC BY license (<http://creativecommons.org/licenses/by/4.0/>).

## 1. Introduction

Homonymous visual field defects (HFVDs) are a common consequence of acquired brain injuries and greatly affect quality of life (Hepworth et al., 2016; Rowe et al., 2013; Suchoff et al., 2008). They cause difficulties in activities such as reading, driving and mobility in general (Das and Huxlin, 2010; De Haan et al., 2015), are associated with emotional disorders such as anxiety and depression (Ali et al., 2013; Wolter and Preda, 2006), and affect

visual memory (Kerckhoff, 2000). Spontaneous recovery does occur but mainly during the first few months after brain injury, and it is rarely complete (Urbanski et al., 2014; Zhang et al., 2006; Zihl, 2000).

Various techniques have been developed to try to improve daily functioning of patients. They can be divided in three major types of therapy: visual restoration therapy, optical aids, and compensation approaches (Lane, 2008).

Restoration techniques have been proposed based on the *residual vision activation theory*; the idea that some visual function can be restored in so-called areas of residual vision (ARVs) - parts of the visual field that are impaired but not completely blind (Sabel

\* Corresponding author.

E-mail address: [aguggis@gmail.com](mailto:aguggis@gmail.com) (A.G. Guggisberg).

et al., 2011). However these techniques only allow for the recovery of a few degrees of visual field and require numerous hours of training (1/2 to 1 hour per day for several months) (Dundon et al., 2015; Urbanski et al., 2014). In other words, they require an extensive investment for a relatively small gain in terms of daily life functioning.

Previous work has suggested some research directions which might lead to more effective restoration approaches in the future.

Behavioral deficits following brain injuries have historically been interpreted in a localizationist framework, and this view was supported by demonstrations of reduced task-related activations of specialized brain regions. However, modern imaging methods have shown that neurological deficits manifest not only during the task, but also during a spontaneous resting-state in form of an impairment of distributed brain networks (Carter et al., 2010; Guggisberg et al., 2019). Neural interactions across brain regions, i.e., functional connectivity (FC), was shown to predict behavioral performance in various tasks. FC measured before the presentation of a stimulus can predict subsequent perception in various modalities (Allaman et al., 2020; Hanslmayr et al., 2005; Sadaghiani et al., 2015; Weisz et al., 2014).

Patients with cerebral pathologies such as stroke and neurodegenerative diseases present a disruption of FC, in particular in alpha-band oscillations, which can be robustly measured even in resting-state recordings and which correlates with the severity of neurological deficits (Adler et al., 2003; Dubovik et al., 2013, 2012). In the case of hemianopia, Pietrelli et al. (2019) reported altered alpha-band oscillation frequency and amplitude over posterior electrodes. In patients with partial optic nerve damage, vision loss is partly caused by synchronization impairments in brain networks, and restitution of alpha band coherence accompanies function recovery (Bola et al., 2015, 2014). Furthermore, disruptions of network interactions have been linked to visual field impairments (Pedersini et al., 2020). Disrupted afferent pathways indeed reduce the input received by the visual cortex. But if the cortex itself is less ready to react to that partial input because of impaired network connectivity, the resulting behavioral deficit would exceed the actual input decrease. Our recent results in healthy subjects support this assumption. In a perithreshold detection task, we showed that subjects displaying the strongest spontaneous FC were those better able to detect the low contrast targets. Furthermore, those subjects actually did not show cortical activations during the task, whereas such activations were found in the subjects that showed less spontaneous FC (Allaman et al., 2020).

Research on HFVDs often focuses on V1 damage. However, injury to other – subcortical – structures of the visual pathway also induces visual field impairment. Any retrochiasmal damage will cause a homonymous defect, even though its congruity can vary (Fraser et al., 2011; Kedar et al., 2007). In these cases, visual impairment is linked to a lack of input rather than a primary malfunction of the visual cortex, which provides a particularly attractive model to test the hypothesis that altered network interaction states in structurally intact brain areas contribute to HFVD severity.

The aim of the present study is thus to examine resting-state network interactions and their influence on task-related neural processes as well as behavioral performance in chronic HFVDs patients due to subcortical, retrochiasmal damage outside of the occipital lobe, and to compare them with matched controls. We expect FC patterns to be impaired in patients, especially for interactions involving the ipsilesional visual cortex. We can furthermore expect that this associates with the visual perception deficit measured behaviorally.

## 2. Materials and methods

### 2.1. Participants

Ten patients with visual field deficits (homologous lateral hemianopsia or quadrantanopsia) after subcortical brain injury but with intact primary visual cortex and ten age and gender-matched control subjects were recruited (see Fig. 1 for the lesions and Table 1 for patient characteristics). Exclusion criteria were ocular diseases, diplopia, hemispatial neglect and inability to fixate precisely during testing. Three additional patients were excluded due to poor quality of the electroencephalography (EEG) recording or excessive sleepiness despite attempts to keep them awake. All patients were in subacute to chronic stages (min. three months after acquired injury) and had undergone ophthalmological and neuropsychological examinations, and compensatory training of eye movements and visual scanning prior to recruitment. All control subjects had normal or corrected-to-normal vision and no history of neurological, ocular or psychiatric disorders and were paid for their participation.

All procedures were approved by the ethical committee of the canton of Geneva and performed according to the declaration of Helsinki. All participants gave written informed consent after receiving explanation on the nature of the experiment.

### 2.2. Procedure

The patients first underwent a visual field assessment with a Humphrey Field Analyzer (HFA) II-I perimetry device (Carl Zeiss Meditec AG, Jena, Germany) that operates with the SITA (Swedish Interactive Thresholding Algorithm) method. Both eyes were tested consecutively with the Central 30–2 protocol. Pupils were not dilated before examination.

A ten-minute eyes-closed resting-state recording was acquired for each subject prior to the task. Then, they were recorded during a passive visual stimulation task with alternating checkerboards. They were seated 60 cm away from a 23.5" Eizo FG2421 liquid-crystal display monitor with a refresh rate of 120 Hz, in a dimly lit room. Stimulus presentation was implemented using E-Prime 2.0 software (Psychology Software Tools, Pittsburgh, PA). The stimulus display occupied 35° of visual angle horizontally and 27° vertically and was composed of four 15x20 checkerboards, one for each quadrant, with a check size of 50 minutes of arc, allowing preferential stimulation of peripheral visual fields (American Clinical Neurophysiology Society, 2006). Michelson contrast was kept above 90%. The central fixation cross took up 2° of visual angle and another 2° separated it from the checkerboard horizontally and vertically, resulting in a 3° wide black band separating the four checkerboards (Fig. 2).

Checkerboards of each quadrant were inverted individually by series of one to three alternating cycles, with a reversal rate of 1 Hz. A pause of one to 1.5 seconds was respected between each quadrant change and the order of quadrants was randomized. A total of 216 reversals were obtained for each quadrant and subject. Subjects were instructed to keep fixation on the fixation cross at all times and to blink minimally. Good fixation was monitored by the experimenter during the task with a video camera transmitting the image of the patient's eyes. Trials with blinks or saccades were subsequently excluded from analysis. The task was divided in six blocks of approximately three minutes each.

### 2.3. Behavioral analyses

To quantify the visual deficit for each patient, we chose to use the Total Deviation values. For each tested point, the Total Devia-

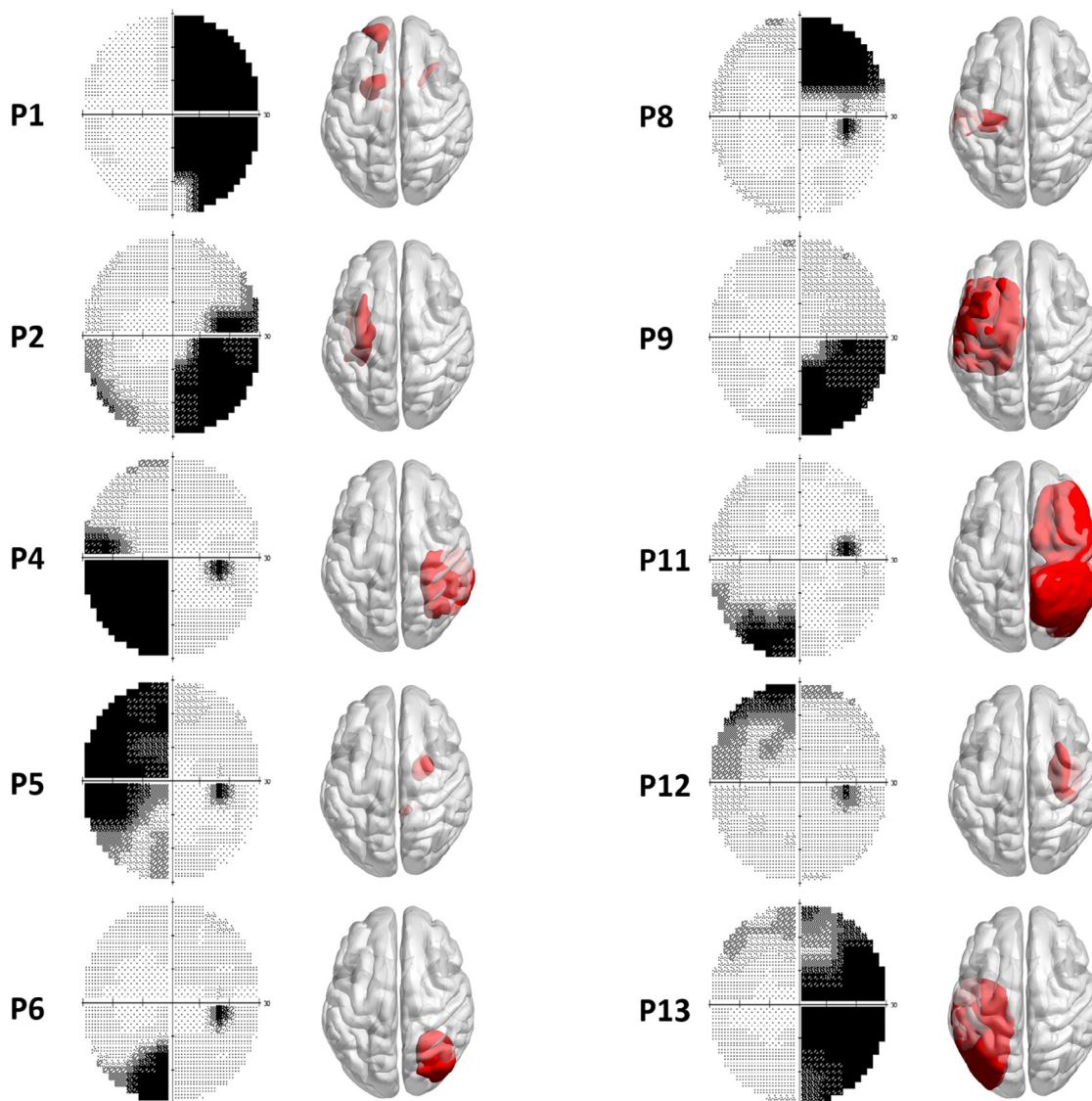


**Fig. 1. Visual field deficits and individual lesion locations.** The evaluated field extended 30 degrees in each direction. Results for the right eye in each patient are depicted. Results for the left eye were globally superimposable. Lesions are visualized on a template brain in neurological convention (left is left).

**Table 1**  
Patient characteristics.

Patient	Age	Gender	Handedness	Side of visual field deficit	Lesion aetiology	Time since lesion (months)	Ocular pathology
P1	38	M	R	R	TBI	8	None
P2	44	M	R	R	H stroke	15	None
P4	22	F	R	L	H stroke	49	None
P5	30	M	R	L	TBI	55	None
P6	37	F	R	L	H stroke	48	None
P8	33	M	R	R	AVM resection	3	None
P9	56	F	R	R	H stroke	51	None
P11	56	F	R	L	I stroke	59	None
P12	57	M	R	L	H stroke	100	None
P13	55	F	R	R	I stroke	3	None

Abbreviations: F = female, M = male, R = right, L = left, TBI = traumatic brain injury, H = hemorrhagic, AVM = arteriovenous malformation, I = ischemic.

tion value gives the difference (in decibels; dB) between the patient’s performance and the normal value for their age, thus enabling us to control for age effects. No further correction was applied for global depression due to ocular pathologies as those were an exclusion criteria for our sample. We averaged the results

obtained for both eyes. For one patient, results from only one eye were used due to poor fixation during the second eye’s testing (blind spot undetectable in the perimetry result). We then computed the mean of all deviation values across the hemifield as index of visual perception for each patient and hemifield.

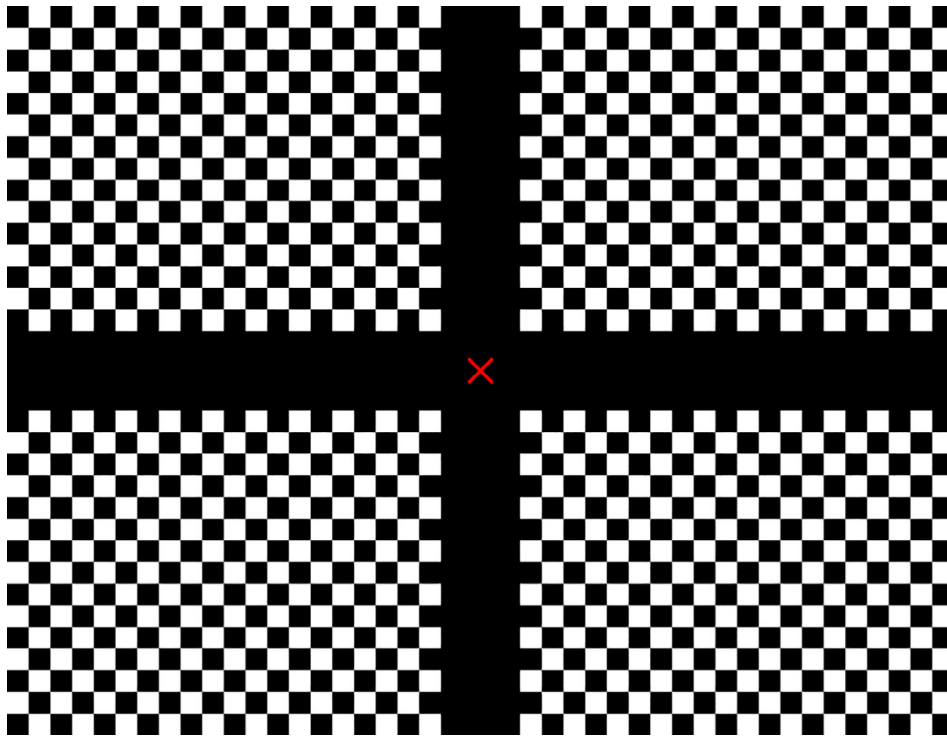


**Fig. 2. Visual stimulus.** Checkerboards of each quadrant were inverted individually at a reversal rate of 1 Hz. See section *Procedure* for details.

#### 2.4. EEG acquisition

EEG data were sampled at 1024 Hz using a 128-channel BioSemi ActiveTwo EEG-system (BioSemi B.V., Amsterdam, Netherlands). Data were re-referenced against the Cz electrode. Artifacts such as eye movements, blinks, power line, and electrode artifacts were removed by visual inspection. The artifact free resting-state data was segmented into non-overlapping 1 s epochs.

#### 2.5. Source imaging

All analyses were performed in MATLAB (The MathWorks, Natick, USA), using the toolbox NUTMEG (Dalal et al., 2011) and its Functional Connectivity Mapping (FCM) toolbox (Guggisberg et al., 2011). Lead-potential was computed using a boundary element head model, with the Helsinki BEM library (Stenroos et al., 2007) and the NUTMEG plugin of NUTMEG (Guggisberg et al., 2011), based on individual T1 MRI or CT-scan when available. When neither was available ( $N = 7$ , all among the control subjects), the BEM model was based on the Montreal Neurological Institute (MNI) template. Gray matter voxels with 10 mm grid spacing were used as solution points. An adaptive filter (scalar minimum variance beamformer) (Sekihara et al., 2004) was used to project the EEG data to the solution points after it had been bandpass-filtered in the respective frequency bands, Hanning windowed and Fourier transformed.

Analysis of FC was conducted as described previously (Guggisberg et al., 2015, 2011). FC was obtained in the  $\alpha$  frequency band (8–12 Hz), where previous studies have consistently found associations with behavior in general (Dubovik et al., 2012; Guggisberg et al., 2015), and with visual perception in particular (Allaman et al., 2020; Pietrelli et al., 2019). To check for band specificity, FC was additionally obtained in the low- $\beta$  (13–20 Hz) and high- $\beta$  (21–30 Hz) bands. The absolute imaginary component of coherence (IC) was computed from 300 artifact-free epochs of 1 s recorded during rest as index of FC. We calculated the weighted

node degree (WND) for each voxel as the sum of its coherence with all other cortical voxels (Newman, 2004). To reduce the influence of differences in signal-to-noise ratio, we normalized WND values by calculating z-scores, by subtracting the mean WND value of all voxels of the subject from the IC values at each voxel and by dividing by the standard deviation over all voxels (Dubovik et al., 2012; Mottaz et al., 2015). WND of regions of interest (ROIs) is computed as the average WND values of all voxels within the ROI.

Task-induced power modulations were calculated for  $\alpha$  as well as low- $\beta$  (13–20 Hz) and high- $\beta$  (21–30 Hz) frequency bands as they show the typical task-induced power decreases that were of interest here (Crone et al., 1998). A 200 ms long sliding window was moved in steps of 50 ms from 100 ms before to 750 ms after checkerboard reversal. Power was computed from a mean of 263 epochs ( $\pm 66$  standard deviation) after stimulation of the left field and 266 epochs ( $\pm 69$ ) after right stimulation using a scalar minimum variance beamformer in the respective windows and frequency bins (Dalal et al., 2008) and log-transformed to decibel (dB) to obtain normal distribution. Baseline power, computed from 300 ms to 100 ms before reversal, was subtracted from power during active time windows. Global power change during the task was obtained as area under curve of all time-windows  $> 300$  ms after reversal (Allaman et al., 2020; Yordanova et al., 2001).

#### 2.6. Statistical analyses

We defined posterior ROIs which are known to be implicated in passive visual perception and spatial attention (e.g., Courtney and Ungerleider, 1997; Wurtz, 2015) from the anatomical automatic labeling (AAL) template (Tzourio-Mazoyer et al., 2002): the primary visual cortex, the superior, middle and inferior occipital gyri, the lingual and fusiform gyri as well as the superior parietal gyrus of both sides. These ROIs were screened for associations between  $\alpha$ -band WND and visual field impairment, as well as between the area under curve of task-induced power modulations in the 3 bands and visual field impairment using Pearson correlations (as

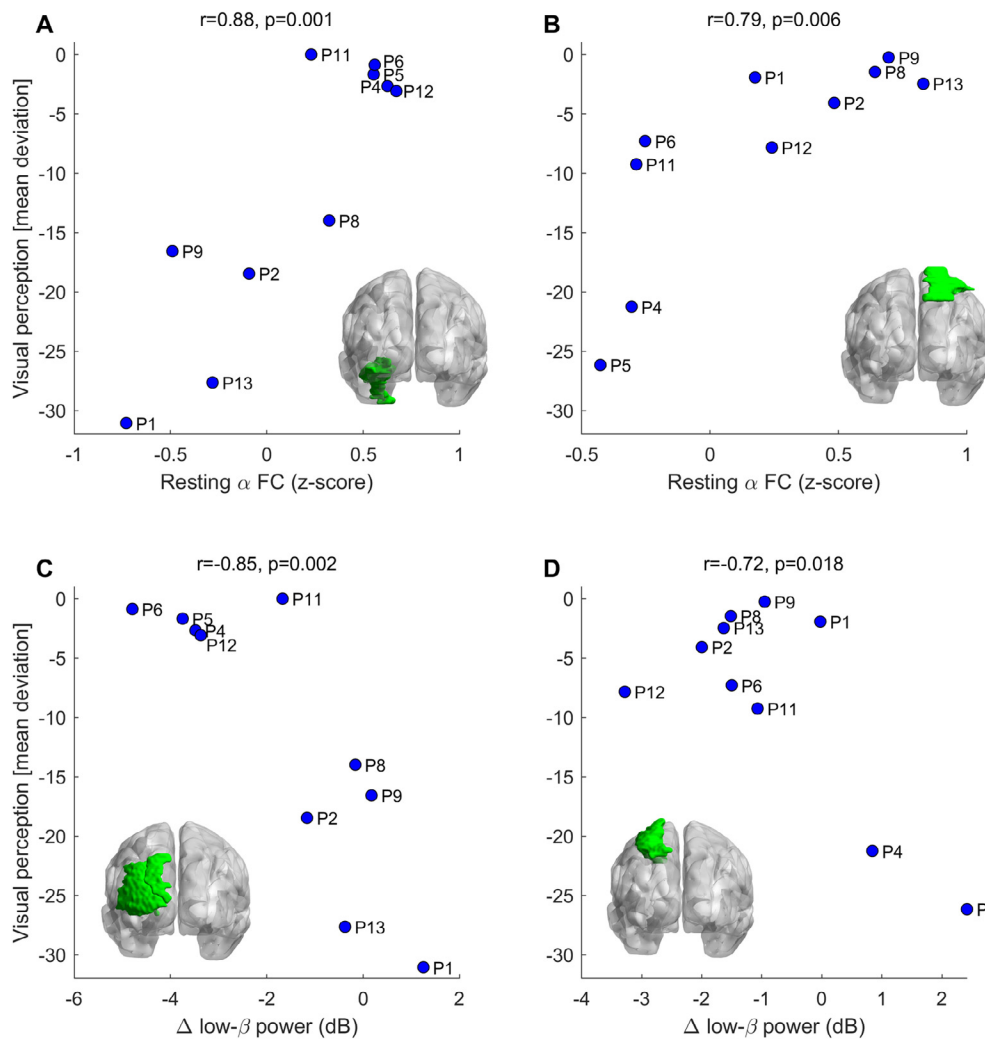


**Fig. 3. Neural correlates of visual impairment.** Patients with greater resting-state  $\alpha$ -weighted node degree of the region of interest showed better visual perception in the contralateral hemifield (A, B, Pearson correlations). Patients with greater low- $\beta$  power decrease showed better visual perception (C, D). FC = Functional Connectivity.

the assumptions of parametric statistics were met). Both hemifields were tested individually. Then, false discovery rate (FDR) correction was applied to adjust for testing multiple ROIs and, in the case of power, frequency bands. Areas with significant associations after correction were then used as ROIs for further analysis. For power changes after left-sided stimulation, no area survived correction, and the area with significant association (uncorrected) was used. The ROIs were visualized with the BrainNet Viewer (<http://www.nitrc.org/projects/bnv/>) (Xia et al., 2013).

To compare WND to power changes at the selected ROIs, they were entered as predictors of visual field impairment in a stepwise regression procedure with forward selection of the best neural feature (FC vs. power). Left and right visual fields were tested in separate regressions. The dependency between WND and power changes was checked with Pearson correlations.

In a second step, for comparison between affected and spared sides and with healthy subjects, the resulting ROIs were relabeled as *ipsilesional* and *contralesional*. For control subjects, we computed the mean of the values obtained in both ROIs (*control*).

The significance of task-induced power modulations was tested with *t*-tests against the null-hypothesis of 0 change, using a cluster correction for testing multiple time–frequency windows. The cluster size threshold was defined by obtaining 500 permutations of the original power values. Each permutation consisted of two

steps: (1) inverting the polarity of the power change values for some subjects (with a different combination of negations in each permutation) and (2) applying *t*-tests on the permuted data and collecting the maximum number of contiguous significant windows in the 2 dimensions of time and frequency. This resulted in an empirical distribution of the number of contiguous time–frequency windows that is obtained by pure chance. The significance of the cluster size obtained in the original data was then calculated from its position within the empirical distribution obtained from permutations. The comparison against maximum cluster size effectively corrects for the familywise error of testing multiple time–frequency windows.

Paired *t*-tests were used to compare FC as well as the area-under-curve of in-task power (for all time windows between 300 and 750 after reversal) in *ipsilesional* vs. *contralesional* ROIs and unpaired *t*-tests to compare patients to controls.

### 3. Results

Perimetry results and individual lesion configurations are illustrated in Fig. 1. Lesions were visualized with the BrainNet Viewer (<http://www.nitrc.org/projects/bnv/>) (Xia et al., 2013). The mean deviations in visual perception from normal values ranged from  $-7.3$  (mild, partial impairment) to  $-31.1$  (complete hemianopia)

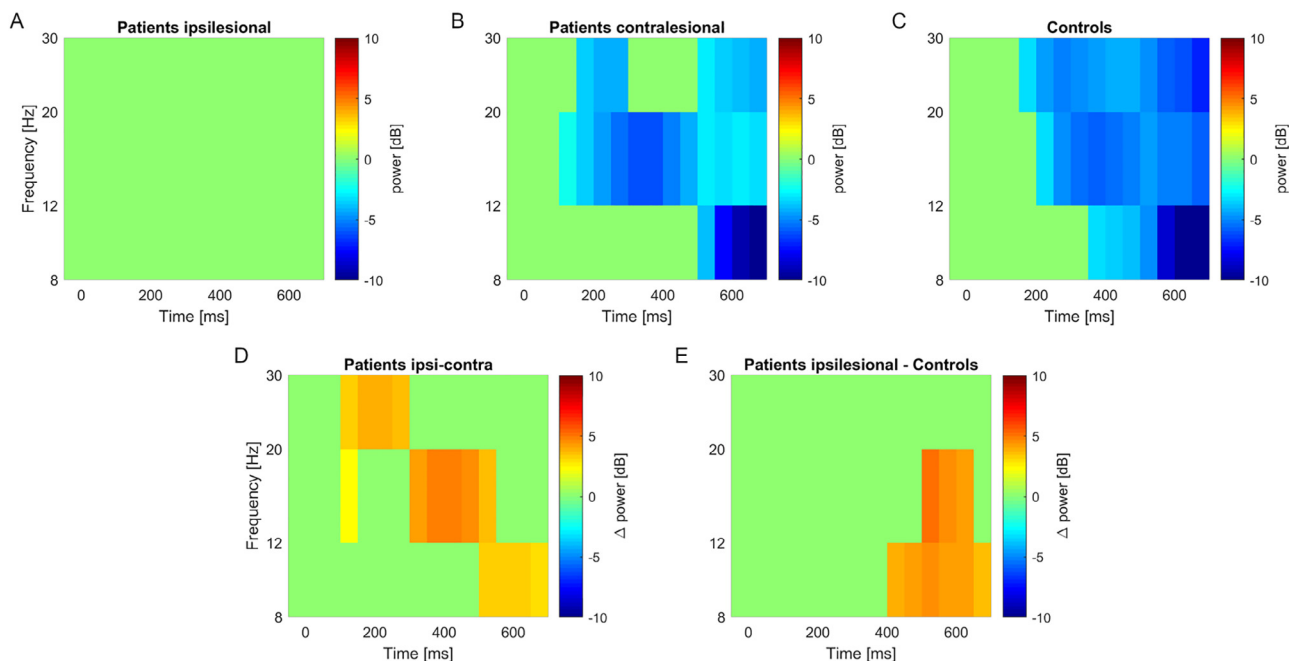


**Fig. 4.** Comparison of task-induced power changes at ipsi- and contralesional sites. Task-induced power change ( $p < 0.05$ , cluster corrected) for patients at the ipsilesional (A), contralesional ROIs (Regions of Interest; B) and for controls (C). Comparison between task-induced power change at the ipsi- and contralesional ROIs in patients ( $p < 0.05$ , cluster corrected) (D). Comparison between task-induced power change at the ipsilesional ROI and controls ( $p < 0.05$ , uncorrected) (E). Time 0 corresponds to checkerboard reversal onset.

dB in the impaired hemifield and from 0 to  $-4.1$  in the spared hemifield.

Visual perception in the right hemifield correlated with  $\alpha$ -WND of the left fusiform gyrus ( $r = 0.88$ ,  $p = 0.005$ , 5% FDR corrected, Fig. 3 C), whereas visual perception in the left hemifield correlated with  $\alpha$ -WND of the right superior parietal gyrus ( $r = 0.79$ ,  $p = 0.045$ , 5% FDR corrected, Fig. 3 D). These correlations were not due to differences in anatomical lesions, as only one patient on each side had the lesion extending to the corresponding ROI. When these patients were excluded, the correlations remained unchanged and highly significant ( $r > 0.83$ ,  $p < 0.0057$ ). Correlations were band-specific and not observed in the low and high  $\beta$  frequency bands on either side ( $r < 0.54$ ,  $p > 0.11$ ). For event-related power decrease, also known as event-related desynchronization (ERD), Low- $\beta$  power decreases at the left superior parietal lobule were associated with less left visual field impairment ( $r = -0.72$ ,  $p = 0.018$ , uncorrected), and low- $\beta$  power at the left superior and middle occipital gyrus with less right field impairment ( $r < -0.82$ ,  $p = 0.041$ , 5% FDR corrected). Again, these ROIs were structurally intact for all except 1 patient showing partial damage. Correlations remained robust when excluding this patient ( $r < -0.71$ ,  $p < 0.031$ ).

A stepwise regression including  $\alpha$ -WND vs. low- $\beta$  power decreases as predictors for the severity of visual field deficits retained only  $\alpha$ -WND for left ( $\beta = 14.7$ ,  $p = 0.006$ ) as well as right ( $\beta = 20.3$ ,  $p = 0.0007$ ) hemi-fields, but not the power change ( $\beta > -2.2$ ,  $p > 0.12$ ). This was because the power change was itself dependent on the  $\alpha$ -WND state at the left ( $r = -0.88$ ,  $p = 0.0007$ ) and right ROI ( $r = -0.56$ ,  $p = 0.094$ ).

These ROIs were then relabeled as *ipsilesional* or *contralesional* for comparison between sides and with controls. The observed task-induced power changes are illustrated in Fig. 4. There was no significant power change from baseline following checkerboard reversal in the impaired ROI (Fig. 4 A). On the other hand, visual stimulation induced a time-frequency cluster of power decreases from baseline in the intact ROI and in controls (Fig. 4 B-C). The cluster-based permutation analysis of power changes further

showed significant differences between impaired and intact ROIs (Fig. 4 D) and between impaired ROI and controls (Fig. 4 E).

Pairwise t-tests confirmed that  $\alpha$ -WND was significantly lower for the ipsilesional ROI ( $p < 0.0001$ ) than contralesional. Unpaired t-tests further showed that ipsilesional  $\alpha$ -WND was also lower than in control subjects ( $p = 0.020$ ) whereas, interestingly, it was higher for the contralesional ROI in patients than in control subjects ( $p = 0.002$ , Fig. 5 A). Task-induced low- $\beta$  power decreases were reduced in ipsilesional ROIs of patients compared to contralesional ROIs ( $p = 0.009$ ) and to control subjects ( $p = 0.013$ ) (Fig. 5 C). Differences in  $\alpha$  and high- $\beta$  bands did not reach significance (Fig. 5 B, D).

#### 4. Discussion

These results demonstrate that network interactions at rest as indexed by  $\alpha$ -WND correlate linearly with visual field impairment following brain lesions. This is in line with previous work that showed strong correlations between disruptions of coherent electrical oscillations at rest and various neurological deficits (Adler et al., 2003; Dubovik et al., 2012), and extends it to visual perception.

We also found reduced/absent ERDs in patients following stimulation of their impaired visual field, in accordance with previous results (Grasso et al., 2020). The intact side, on the other hand shows a similar reaction to stimulation to control subjects. However, inter-individual differences in ERD depended themselves on the level of spontaneous  $\alpha$ -WND, such that only patients with higher level of spontaneous interactions were able to generate activations as indexed by ERD. Furthermore, when using multivariate regressions, only spontaneous  $\alpha$ -WND, but not ERDs, were retained as predictors for the level of visual field loss. This may seem surprising at first glance but goes well with our recent results on healthy subjects that showed that resting-state FC was a better predictor of visual perception than task-related power changes (Allaman et al., 2020).

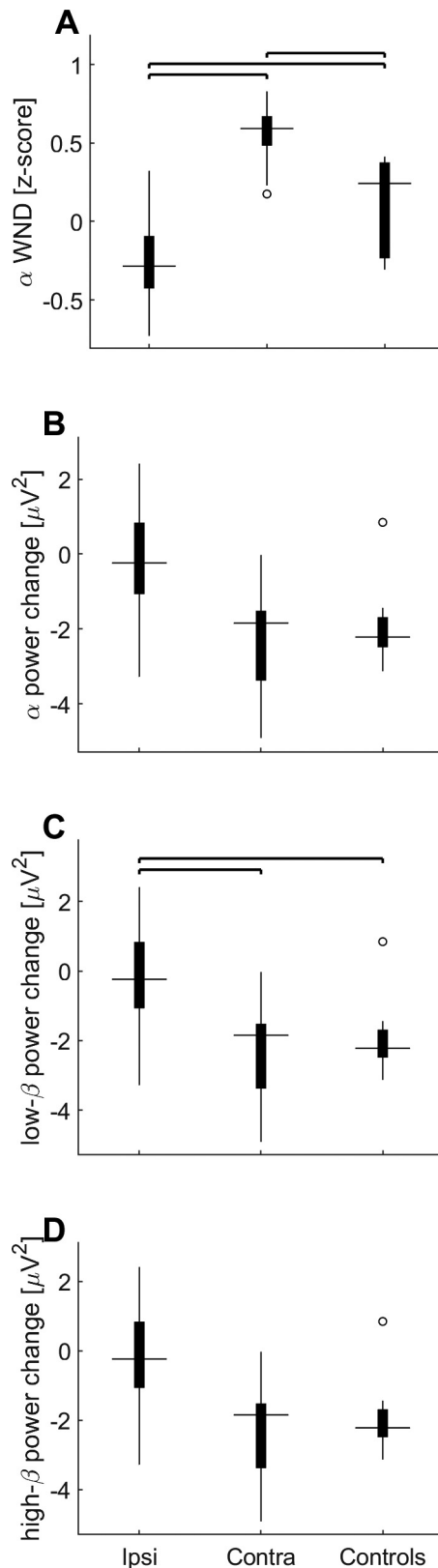


**Fig. 5. Comparison of neural markers at ipsi- and contralesional ROIs in patients and in controls.** Comparison of  $\alpha$ -WND (weighted node degree; A). Comparison of area under the curve of task-induced power changes at  $\alpha$ , low- $\beta$ , and high- $\beta$  frequency bands (B–D). Horizontal lines indicate significant differences at  $p < 0.05$ .

New techniques for neurological rehabilitation include neuro-modulation approaches such as neurofeedback training. One of the targets for neuromodulation is amplitude of low frequency activity (Bearden et al., 2003; Hsueh et al., 2016; Orzechowski et al., 2015; Zoefel et al., 2011). However, our results suggest that FC would be a more relevant target for such intervention.  $\alpha$ -WND has previously been successfully trained in healthy subjects and stroke patients, and led to an behavioral improvement in the latter (Mottaz et al., 2018, 2015).

HFVDs are classically categorized as pure sensory deficits, as opposed to, for example, attentional disorders such as neglect. However, we found that resting-state network interactions of the right superior parietal cortex, a brain region classically associated with top-down control of visuo-spatial attention (Gillebert et al., 2011), were associated with visual perception in our patients. It has previously been pointed out that the role of attention in HFVDs and their rehabilitation has been underestimated. Indeed, Lane and colleagues (Lane et al., 2010) showed that attention training with stimuli presented in the central 2° of the visual field yielded performance enhancements in a variety of vision-related task – including perimetry – that were of similar magnitude as those obtained following visual exploration training. The authors suggest that attending to locations in the “blind” visual field increases the excitability of preserved neurons in the corresponding visual cortex. By enhancing the patients’ ability to direct their focus, attention training allowed them to lower their detection threshold in the attended location. These top-down influences of visual might further influence the network interaction states of visual areas. The ability to measure such effects will then provide insights into the neurophysiological mechanisms underlying attention treatment.

Concerning patients with left sided lesions, it was the WND of the left fusiform gyrus that correlated with the visual field deficit. Classically, the fusiform gyrus is associated with object recognition in general and faces in particular (McCarthy et al., 1997) as well as words for the left fusiform gyrus (McCandliss et al., 2003). However, it was shown that the level of coupling between V1 and the fusiform cortex was linked to stimulus visibility (Haynes et al., 2005). This supports the notion that feedback from higher order visual areas mediates visual awareness.

It may seem surprising that we found asymmetrical results between left- and right-brain damaged patients. A possible explanation lies in the well-established right hemisphere dominance for attentional processing (Heilman and Van Den Abell, 1980). Indeed, it is thought to play a role in bilateral attentional deficits following right parietal and occipital lesions (Chokron et al., 2019). Attentional processes might then play a more important role in visual field deficits following right than left brain damage, which themselves would be more strongly related to perceptual processes.

We also found an excess in FC in the intact ROI as compared to healthy subjects. This phenomenon has already been observed for contralesional brain regions following stroke (Dubovik et al., 2012). In the specific case of visual field impairment, this is of particular interest. Indeed the ipsilesional visual field has classically been considered as fully “intact” and was not assessed beyond the results of perimetry evaluation. However, recent research identified perceptual deficits in the ipsilesional visual field of hemianopic patients, the so-called “sightblindness” phenomenon (Bola et al., 2013). Interestingly, the nature of those deficits differs depending on lesion side (Cavézien et al., 2010). Perceptual deficits in the seeing visual field could account for part of the “mismatch problem”, the fact that a subjective improvement perceived by patients can occur without an actual expansion of the visual field tested by

perimetry and conversely that an enlargement of visual field can go unnoticed by the patient (Sabel et al., 2011). Network interactions involving the contralesional visual cortex may be involved in sightblindness.

One of the limitation of this work is that no cerebral imaging was available for the controls subjects. We also did not formally test the control subjects' perimetry, which were assumed normal given their medical history. Therefore, although none had a history of neurological symptoms, we cannot totally exclude the possibility of cerebral lesions in the control group. However, if this were the case, it would have reduced the observed differences reported here, which would then in reality be even larger.

In conclusion, our findings demonstrate that visual field deficits following brain lesions associate not only with a lack of activation during visual tasks, but also with a loss of spontaneous neural interactions. This may open new treatment targets in the future.

## Funding

This work has been supported by the Swiss National Science Foundation (grant 320030\_169275 to AGG).

## Declaration of Competing Interest

The authors declare that they have no known competing financial interests or personal relationships that could have appeared to influence the work reported in this paper.

## Acknowledgments

We would like to thank Prof. Radek Ptak for help with methodological aspects.

## References

- Adler G, Brassens S, Jajcevic A. EEG coherence in Alzheimer's dementia. *J Neural Transm* 2003;110:1051–8. <https://doi.org/10.1007/s00702-003-0024-8>.
- Ali M, Hazelton C, Lyden P, Pollock A, Brady M. Recovery from poststroke visual impairment: Evidence from a clinical trials resource. *Neurorehabil Neural Repair* 2013;27:133–41. <https://doi.org/10.1177/1545968312454683>.
- Allaman L, Mottaz A, Kleinschmidt A, Guggisberg AG. Spontaneous network coupling enables efficient task performance without local task-induced activations. *J Neurosci* 2020. <https://doi.org/10.1523/JNEUROSCI.1166-20.2020>.
- Bearden TS, Cassisi JE, Pineda M. Neurofeedback training for a patient with thalamic and cortical infarctions. *Appl Psychophysiol Biofeedback* 2003;28:241–53. <https://doi.org/10.1023/A:1024689315563>.
- Bola M, Gall C, Moewes C, Fedorov A, Hinrichs H, Sabel BA. Brain functional connectivity network breakdown and restoration in blindness. *Neurology* 2014;83:542–51. <https://doi.org/10.1212/WNL.0000000000000672>.
- Bola M, Gall C, Sabel BA. Disturbed temporal dynamics of brain synchronization in vision loss. *Cortex* 2015;67:134–46. <https://doi.org/10.1016/j.cortex.2015.03.020>.
- Bola M, Gall C, Sabel BA. "Sightblind": Perceptual deficits in the "intact" visual field. *Front Neurol* 2013;4 JUN:1–5. <https://doi.org/10.3389/fneur.2013.00080>.
- Carter AR, Astafiev SV, Lang CE, Connor LT, Rengachary J, Strube MJ, et al. Resting interhemispheric functional magnetic resonance imaging connectivity predicts performance after stroke. *Ann Neurol* 2010;67:365–75. <https://doi.org/10.1002/ana.21905>.
- Cavézián C, Gaudry I, Perez C, Coubard O, Doucet G, Peyrin C, et al. Specific impairments in visual processing following lesion side in hemianopic patients. *Cortex* 2010;46:1123–31. <https://doi.org/10.1016/j.cortex.2009.08.013>.
- Chokron S, Peyrin C, Perez C. Ipsilesional deficit of selective attention in left homonymous hemianopia and left unilateral spatial neglect. *Neuropsychologia* 2019;128:305–14. <https://doi.org/10.1016/j.neuropsychologia.2018.03.013>.
- Courtney SM, Ungerleider LG. What fMRI has taught us about human vision. *Curr Opin Neurobiol* 1997;7:554–61. [https://doi.org/10.1016/S0959-4388\(97\)80036-0](https://doi.org/10.1016/S0959-4388(97)80036-0).
- Crone NE, Miglioretti DL, Gordon B, Sieracki JM, Wilson MT, Uematsu S, et al. Functional mapping of human sensorimotor cortex with electrocorticographic spectral analysis. I. Alpha and beta event-related desynchronization. *Brain* 1998;121:2271–99.
- Dalal SS, Guggisberg AG, Edwards E, Sekihara K, Findlay AM, Canolty RT, et al. Five-dimensional neuroimaging: Localization of the time-frequency dynamics of cortical activity. *Neuroimage* 2008;40:1686–700. <https://doi.org/10.1016/j.neuroimage.2008.01.023>.
- Dalal SS, Zumer JM, Guggisberg AG, Trumpis M, Wong DDE, Sekihara K, et al. MEG/EEG Source Reconstruction, Statistical Evaluation, and Visualization with NUTMEG. *Comput Intell Neurosci* 2011;2011:758973. <https://doi.org/10.1155/2011/758973>.
- Das A, Huxlin KR. New approaches to visual rehabilitation for cortical blindness: outcomes and putative mechanisms. *Neuroscientist* 2010;16:374–87. <https://doi.org/10.1177/1073858409356112>.
- Dubovik S, Pignat JM, Ptak R, Aboulafia T, Allet L, Gillibert N, et al. The behavioral significance of coherent resting-state oscillations after stroke. *Neuroimage* 2012;61:249–57. <https://doi.org/10.1016/j.neuroimage.2012.03.024>.
- Dubovik S, Ptak R, Aboulafia T, Magnin C, Gillibert N, Allet L, et al. EEG alpha band synchrony predicts cognitive and motor performance in patients with ischemic stroke. *Behav Neurol* 2013;26:187–9. <https://doi.org/10.3233/BEN-2012-129007>.
- Dundon NM, Bertini C, Ládavas E, Sabel BA, Gall C. Visual rehabilitation: visual scanning, multisensory stimulation and vision restoration trainings. *Front Behav Neurosci* 2015;9:1–14. <https://doi.org/10.3389/fnbeh.2015.00192>.
- Fraser JA, Newman NJ, Biousse V. Disorders of the optic tract, radiation, and occipital lobe. *Handb Clin Neurol* 2011;102:205–21. <https://doi.org/10.1016/B978-0-444-52903-9.00014-5>.
- Gillibert CR, Mantini D, Thijs V, Sunaert S, Dupont P, Vandenberghe R. Lesion evidence for the critical role of the intraparietal sulcus in spatial attention. *Brain* 2011;134:1694–709. <https://doi.org/10.1093/brain/awr085>.
- Grasso PA, Pietrelli M, Zanon M, Ládavas E, Bertini C. Alpha oscillations reveal implicit visual processing of motion in hemianopia. *Cortex* 2020;122:81–96. <https://doi.org/10.1016/j.cortex.2018.08.009>.
- Guggisberg AG, Dalal SS, Zumer JM, Wong DD, Dubovik S, Michel CM, et al. Localization of cortico-peripheral coherence with electroencephalography. *Neuroimage* 2011;57:1348–57. <https://doi.org/10.1016/j.neuroimage.2011.05.076>.
- Guggisberg AG, Koch PJ, Hummel FC, Buetefisch CM. Brain networks and their relevance for stroke rehabilitation. *Clin Neurophysiol* 2019;130:1098–124. <https://doi.org/10.1016/j.clinph.2019.04.004>.
- Guggisberg AG, Rizk S, Ptak R, Di Pietro M, Saj A, Lazeyras F, et al. Two Intrinsic Coupling Types for Resting-State Integration in the Human Brain. *Brain Topogr* 2015;28:318–29. <https://doi.org/10.1007/s10548-014-0394-2>.
- De Haan GA, Heutink J, Melis-Dankers BJM, Brouwer WH, Tucha O. Difficulties in daily life reported by patients with homonymous visual field defects. *J Neuro-Ophthalmology* 2015;35:259–64. <https://doi.org/10.1097/WNO.0000000000000244>.
- Hanslmayr S, Klimesch W, Sauseng P, Gruber W, Doppelmayr M, Freunberger R, et al. Visual discrimination performance is related to decreased alpha amplitude but increased phase locking. *Neurosci Lett* 2005;375:64–8. <https://doi.org/10.1016/j.neulet.2004.10.092>.
- Haynes JD, Driver J, Rees G. Visibility reflects dynamic changes of effective connectivity between V1 and fusiform cortex. *Neuron* 2005;46:811–21. <https://doi.org/10.1016/j.neuron.2005.05.012>.
- Heilman KM, Van Den Abell T. Right hemisphere dominance for attention: The mechanism underlying hemispheric asymmetries of inattention (neglect). *Neurology* 1980;30:327–30. <https://doi.org/10.1212/wnl.30.3.327>.
- Hepworth LR, Rowe FJ, Walker MF, Rockliffe J, Noonan C, Howard C, et al. Post-stroke Visual Impairment: A Systematic Literature Review of Types and Recovery of Visual Conditions. *Ophthalmol Res An Int J* 2016:1–43.
- Hsueh J-J, Chen T-S, Chen J-J, Shaw F-Z. Neurofeedback training of EEG alpha rhythm enhances episodic and working memory. *Hum Brain Mapp* 2016;37:2662–75. <https://doi.org/10.1002/hbm.23201>.
- Kedar S, Zhang X, Lynn MJ, Newman NJ, Biousse V. Congruency in Homonymous Hemianopia. *Am J Ophthalmol* 2007;143:772–80. <https://doi.org/10.1016/j.ajo.2007.01.048>.
- Kerkhoff G. Neurovisual rehabilitation: Recent developments and future directions. *J Neurol Neurosurg Psychiatry* 2000;68:691–706. <https://doi.org/10.1136/jnnp.68.6.691>.
- Lane A. Clinical treatment options for patients with homonymous visual field defects. *Clin Ophthalmol* 2008;2:93. <https://doi.org/10.2147/oph.s2371>.
- Lane AR, Smith DT, Ellison A, Schenk T. Visual exploration training is no better than attention training for treating hemianopia. *Brain* 2010;133:1717–28. <https://doi.org/10.1093/brain/awq088>.
- McCandliss BD, Cohen L, Dehaene S. The visual word form area: Expertise for reading in the fusiform gyrus. *Trends Cogn Sci* 2003;7:293–9. [https://doi.org/10.1016/S1364-6613\(03\)00134-7](https://doi.org/10.1016/S1364-6613(03)00134-7).
- McCarthy G, Puce A, Gore JC, Allison T. Face-specific processing in the human fusiform gyrus. *J Cogn Neurosci* 1997;9:605–10. <https://doi.org/10.1162/jocn.1997.9.5.605>.
- Mottaz A, Corbet T, Doganci N, Magnin C, Nicolo P, Schnider A, et al. Modulating functional connectivity after stroke with neurofeedback: Effect on motor deficits in a controlled cross-over study. *Neuroimage Clin* 2018;20:336–46. <https://doi.org/10.1016/j.nicl.2018.07.029>.
- Mottaz A, Solcà M, Magnin C, Corbet T, Schnider A, Guggisberg AG. Neurofeedback training of alpha-band coherence enhances motor performance. *Clin Neurophysiol* 2015;126:1754–60. <https://doi.org/10.1016/j.clinph.2014.11.023>.
- Newman MEJ. Analysis of weighted networks. *Phys Rev E Stat Nonlin Soft Matter Phys* 2004;70:56131. <https://doi.org/10.1103/PhysRevE.70.056131>.

- Orzechowski G, Jurewicz K, Paluch K. Brain-training for physical performance: A study of EEG-neurofeedback and alpha relaxation training in athletes. *Acta Neurobiol Exp (Wars)* 2015;75:434–45.
- Pedersini CA, Guardia-Olmos J, Montala-Flaquer M, Cardobi N, Sanchez-Lopez J, Parisi G, et al. Functional interactions in patients with hemianopia: A graph theory-based connectivity study of resting fMRI signal. *PLoS One* 2020;15. <https://doi.org/10.1371/journal.pone.0226816> e0226816.
- Pietrelli M, Zanon M, Ládavas E, Grasso PA, Romei V, Bertini C. Posterior brain lesions selectively alter alpha oscillatory activity and predict visual performance in hemianopic patients. *Cortex* 2019;121:347–61. <https://doi.org/10.1016/j.cortex.2019.09.008>.
- Rowe FJ, Wright D, Brand D, Jackson C, Harrison S, Maan T, et al. A Prospective Profile of Visual Field Loss following Stroke: Prevalence, Type, Rehabilitation, and Outcome. *Biomed Res Int* 2013;2013. <https://doi.org/10.1155/2013/719096> 719096.
- Sabel BA, Henrich-Noack P, Fedorov A, Gall C. Vision restoration after brain and retina damage: The “residual vision activation theory”. *Prog Brain Res* 2011;192:199–262. <https://doi.org/10.1016/B978-0-444-53355-5.00013-0>.
- Sadaghiani S, Poline J-B, Kleinschmidt A, D’Esposito M. Ongoing dynamics in large-scale functional connectivity predict perception. *Proc Natl Acad Sci* 2015;112:8463–8. <https://doi.org/10.1073/pnas.1420687112>.
- Sekihara K, Nagarajan SS, Poeppel D, Marantz A. Asymptotic SNR of scalar and vector minimum-variance beamformers for neuromagnetic source reconstruction. *IEEE Trans Biomed Eng* 2004;51:1726–34. <https://doi.org/10.1109/TBME.2004.827926>.
- Stenroos M, Mantynen V, Nenonen J. A Matlab library for solving quasi-static volume conduction problems using the boundary element method. *Comput Methods Programs Biomed* 2007;88:256–63. <https://doi.org/10.1016/j.cmpb.2007.09.004>.
- Suchoff IB, Kapoor N, Ciuffreda KJ, Rutner D, Han E, Craig S. The frequency of occurrence, types, and characteristics of visual field defects in acquired brain injury: A retrospective analysis. *Optometry* 2008;79:259–65. <https://doi.org/10.1016/j.optm.2007.10.012>.
- Tzourio-Mazoyer N, Landeau B, Papathanassiou D, Crivello F, Etard O, Delcroix N, et al. Automated anatomical labeling of activations in SPM using a macroscopic anatomical parcellation of the MNI MRI single-subject brain. *Neuroimage* 2002;15:273–89. <https://doi.org/10.1006/nimg.2001.0978>.
- Urbanski M, Coubarde OA, Bourlon C, Urbanski M, Urbanski M. Visualizing the blind brain: Brain imaging of visual field defects from early recovery to rehabilitation techniques. *Front Integr Neurosci* 2014;8:74. <https://doi.org/10.3389/fnint.2014.00074>.
- Weisz N, Wühle A, Monittola G, Demarchi G, Frey J, Popov T, et al. Prestimulus oscillatory power and connectivity patterns predispose conscious somatosensory perception. *Proc Natl Acad Sci U S A* 2014;111. <https://doi.org/10.1073/pnas.1317267111>.
- Wolter M, Preda S. Visual deficits following stroke: Maximizing participation in rehabilitation. *Top Stroke Rehabil* 2006;13:12–21. <https://doi.org/10.1310/3JRY-B168-5N49-XOWA>.
- Wurtz RH. Using perturbations to identify the brain circuits underlying active vision. *Philos Trans R Soc B Biol Sci* 2015;370. <https://doi.org/10.1098/rstb.2014.0205>.
- Xia M, Wang J, He Y. BrainNet Viewer: A Network Visualization Tool for Human Brain Connectomics. *PLoS One* 2013;8. <https://doi.org/10.1371/journal.pone.0068910>.
- Yordanova J, Kolev V, Polich J. P300 and alpha event-related desynchronization (ERD). *Psychophysiology* 2001;38:143–52. <https://doi.org/10.1111/1469-8986.3810143>.
- Zhang X, Kedar S, Lynn MJ, Newman NJ, Biouesse V. Natural history of homonymous hemianopia. *Neurology* 2006;66:901–5. <https://doi.org/10.1212/01.wnl.0000203338.54323.22>.
- Zihl J. *Rehabilitation of visual disorders after brain injury*. East Sussex, UK: Psychology Press; 2000.
- Zoefel B, Huster RJ, Herrmann CS. Neurofeedback training of the upper alpha frequency band in EEG improves cognitive performance. *Neuroimage* 2011;54:1427–31. <https://doi.org/10.1016/j.neuroimage.2010.08.078>.